LBL-29732
Preprint

Lawrence Berkeley Laboratory
UNIVERSITY OF CALIFORNIA

Submitted to Zeitschrift für Physik

Nuclear Rotational Population Patterns in Heavy Ion Scattering and Transfer Reactions

J.O. Rasmussen, M.A. Stoyer, L.F. Canto, R. Donangelo, and P. Ring

October 1990

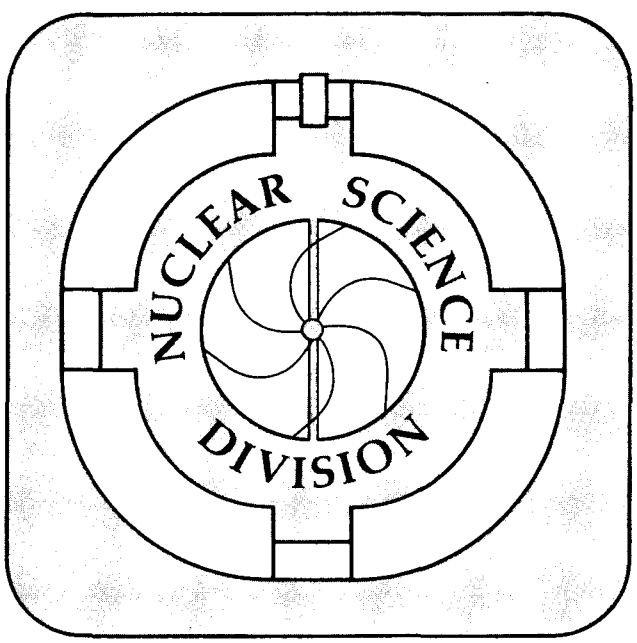

LBL-29732
Copy 2
Bldg. 50 Library.
LOAN COPY
Circulates
for 2 weeks

Prepared for the U.S. Department of Energy under Contract Number DE-AC03-76SF00098

DISCLAIMER

This document was prepared as an account of work sponsored by the United States Government. While this document is believed to contain correct information, neither the United States Government nor any agency thereof, nor the Regents of the University of California, nor any of their employees, makes any warranty, express or implied, or assumes any legal responsibility for the accuracy, completeness, or usefulness of any information, apparatus, product, or process disclosed, or represents that its use would not infringe privately owned rights. Reference herein to any specific commercial product, process, or service by its trade name, trademark, manufacturer, or otherwise, does not necessarily constitute or imply its endorsement, recommendation, or favoring by the United States Government or any agency thereof, or the Regents of the University of California. The views and opinions of authors expressed herein do not necessarily state or reflect those of the United States Government or any agency thereof or the Regents of the University of California.

LBL - 29732

Nuclear Rotational Population Patterns in Heavy Ion Scattering and Transfer Reactions

J.O. Rasmussen, M.A. Stoyer, L.F. Canto, R. Donangelo, and P. Ring

Nuclear Science Division, Lawrence Berkeley Laboratory
University of California, Berkeley, California 94720, USA

October 1990

This work was supported by the Director, Office of Energy Research, Division of Nuclear Physics of the Office of High Energy and Nuclear Physics of the U.S. Department of Energy under Contract DE-AC03-76SF00098

Manuscript for Zeitschrift für Physik edition
honoring the 60th birthday of Professor Hans-Jörg Mang
Berkeley, 15 October, 1990

Nuclear Rotational Population Patterns in Heavy-Ion Scattering and Transfer Reactions

John O. Rasmussen and Mark A. Stoyer
University of California
Lawrence Berkeley Laboratory
Berkeley, CA 94720

L. Felipe Canto and Raul Donangelo
Univ. Fed. do Rio de Janeiro
Rio de Janeiro, Brazil

and

Peter Ring
Tech. Univ. München
Garching, Germany

ABSTRACT

A model of ^{239}Pu with decoupled neutron is used for theoretical calculations of rotational population patterns in heavy ion inelastic scattering and one-neutron transfer reactions. The system treated is ^{90}Zr on ^{239}Pu at the near-barrier energy of 500 MeV and backscattering angles of 180° and 140°. The influence of the complex nuclear optical potential is seen to be very strong, and the Nilsson wave function of the odd neutron produces a distinctive pattern in the transfer reaction.

Introduction

Hans Jörg Mang's pioneering work on the microscopic shell-model approach to alpha decay rate theory for spherical nuclei [1] set the stage for a microscopic theory of rotational population patterns in alpha decay [2]. The essential connection is that on the nuclear surface alpha decay amplitudes to various rotational states are simply the spherical harmonic expansion coefficients of the alpha wave on the nuclear surface. These amplitudes are somewhat modified on passage through the Coulomb barrier, with the barrier transmission handled either by coupled-channel calculations [3] or more often by simpler approximations, such as, the Fröman matrix method [4]. Conversely, the rotational population patterns contain information about the alpha wave function on the nuclear surface, but the relationship is analogous to that of X-ray diffraction spot intensities to a crystal structure. That is, rotational group intensities and X-ray spot intensities are both squares of amplitudes, which may have either of two signs. One must guess, use models, or other tricks to assign the signs in order to work backwards from experiment.

Nucleon transfer reactions on deformed nuclei have revealed, for example, the Nilsson coefficients of neutron wave functions. The case of (d,p) and (d,t) reactions on even-even spheroidal nuclei is especially simple to interpret, as the intensities to particular rotational states give directly the probability of that j value within the Nilsson wave function of the odd neutron [5].

The theoretical calculation of rotational population patterns for neutron transfer reactions with heavy ions is more complicated than the deuteron-induced transfer, since there can be considerable Coulomb excitation on both the inward and outward path. This extra richness in heavy-ion transfer makes the reaction a spectroscopic tool, allowing

exploration of higher rotational states than might otherwise be accessible [6]. In particular this tool may have special value in the actinide region, where the paucity of sufficiently long-lived isotopes for targets limits the cases for pure Coulomb excitation. Furthermore, fission competition complicates the study of high rotational states by (heavy-ion, xn) reactions. For example, ^{58}Ni ions on a ^{235}U target revealed [7] ^{234}U ground band transitions up to spin 26+.^{90}Zr ions on ^{239}Pu at 500 MeV (lab) excited many rotational transitions in ^{238}Pu [8].

In this paper we make a first attempt at a theoretical calculation of the ^{239}Pu neutron pickup reaction case mentioned above. To simplify the Coulomb excitation part, we do the calculation on the even-even core ^{238}Pu, assuming the rotational energy limit of completely decoupled odd neutron to relate the populations to ^{239}Pu. The odd neutron is in the $\frac{1}{2}^+$ [631] Nilsson state and is only mildly coupled to the core, so the error in energy levels with this assumption should not greatly affect the rotation population in ^{239}Pu, since even the sudden approximation with implicit zero rotational spacing should be fairly good in this case. It is not practical for neutron-transfer experiments, where the experiment is run at energies slightly above the Coulomb barrier, to ignore the nuclear optical potential effects. Usually the Alder Winther-deBoer Coulomb excitation codes [9] do not incorporate nuclear potential effects. However, in a recent paper we have shown [10] that their approach can be modified to take into account effects of the real and imaginary parts of a deformed nuclear optical potential; the results compared well for the system of ^{40}Ar on ^{160}Gd with the fully quantum mechanical coupled-channels calculations of Rhoades-Brown et al.[11] Our modifications in ref. [10] are to expand the complex nuclear potential in spherical harmonic

terms added to the normal quadrupole and hexadecapole electromagnetic terms. Though we leave the classical trajectory in hyperbolic Rutherford form, we introduce effective energy and charge values such that the classical turning radius, and radial force at that point for equivalent spherical nuclei are correct, taking into account the real part of the nuclear potential. It is important to point out that our present version of Alder-Winther-deBoer type codes compute for 180° backward scattering, as do the comparison quantum-mechanical coupled-channels and Classical Limit S-Matrix codes. We correct for other scattering angles by adjusting the effective bombarding energy to match the distance of closest approach for the given scattering angle. However, this simplification, allowing us to consider only $M=0$ rotational state amplitudes, is not an essential one and can be later generalized to arbitrary scattering angles.

Rotational Inelastic Scattering Results

We show in Fig. 1 the results at three different beam energies for pure Coulomb excitation, without the nuclear potential. The rainbow maximum at high spin is seen, with the familiar interference oscillations going down to lower spin and the exponential fall-off of intensity above the rainbow maximum. To apply these results to ^{239}Pu under the approximation described above we divide each ^{238}Pu level intensity between the two corresponding levels in ^{239}Pu according to the statistical weight. That is, the spin-0 population all goes to spin 1/2 in ^{239}Pu. The spin-2 population divides between spin 3/2 and spin 5/2 in the ratio of 4 to 6, and so on. Fig. 2 shows how this approximation compares favorably with a complete odd-A Coulomb excitation calculation. In the limit of zero

rotational spacing and complete decoupling the results would be identical. The ^{239}Pu moment of inertia is so large that the approximation is quite good. The odd-neutron coupling is sufficiently small to ignore core rotational motion in the initial state.

Introduction of the complex deformed nuclear optical potential by the methods of ref. [10] makes a profound difference at a near-barrier energy, as is clear from Fig. 3. The rainbow maximum and interference oscillations are gone. For this calculation we have used effectively a slightly lower energy than the 500 MeV head-on calculation of Fig.2, to take into account the mean scattering angle of 140° in an experiment done with this system. (We do not plot the partitioning of intensities into the levels of ^{239}Pu, since that is easily enough done and would result in the same general monotonic decline of intensity with spin down from a maximum at the 5/2 level.) We can rationalize the nuclear potential effects by thinking in terms of the earlier theoretical approaches of the Classical Limit S-Matrix (CLSM). In the CLSM method the rainbow maximum comes from collisions with the spheroidal nucleus oriented about 45 degrees to the point of closest approach, that is, encounters with the perigee in the mid North and South temperate latitudes of the nuclear spheroid. Introduction of an attractive real component of the nuclear potential means that the Coulomb torque has a destructive interference, and that the torque may even reverse sign at short distances, pushing rotational population back to lower spins. Introduction of an imaginary absorptive component in the optical potential means the removal of flux for the higher latitudes, where the perigee comes too close to the prolate nuclear surface. As the energy comes to be above the barrier for equivalent spherical nuclei the only surviving trajectories are those with perigee near the equator, where the quadrupole torque is small, and only low spins are excited.

Neutron Transfer Rotational Population Patterns

To calculate rotational populations for the 1-neutron transfer reaction we resort to a method that we had explored also for the handling of nuclear potential effects for inelastic scattering. That is, we integrate the time-dependent coupled Schrödinger equations of Alder-Winther-deBoer form inward to closest approach. The vector of complex rotational amplitudes is at that point multiplied by a square matrix for the short-range effects under consideration. Then the resultant amplitude vector is further integrated along the outward path of the collision partners.

Canto et al. [12] derived expressions for latitude-dependent factors over the nuclear surface for transfer reactions. One such factor is a_{abs}, the amplitude factor for survival from absorption by the imaginary part of the optical potential. This factor depends on the polar angle of closest approach on the nuclear spheroid.

$$a_{abs}(x) = \exp\{C \exp[\frac{R(x)}{a_w}]\} \tag{1}$$

where a_w = 0.54 fm (the optical potential diffuseness), $x = \cos\theta$, R(x) is the closest separation of the nuclear surfaces.

$$C = -\frac{W_0}{\hbar}\sqrt{\frac{8\mu\pi a^2 a_w}{Z_p Z_t e^2}} \tag{2}$$

where a is half the distance of closest approach and W_0 is the strength of the imaginary optical potential. We argue in the following that the a_{tun} factor of ref. [10] will be nearly constant with angle, and we replace it by unity. The Nilsson single-oscillator-shell expansion is best interpreted as an expansion on a spheroid of half the eccentricity of the deformed constant-density nuclear surface. The classical turning surface for the heavy ion collision is also a prolate surface due to the electric quadrupole potential. Hence, the tunneling distance will be nearly constant at energies near barrier.

The "spectator" odd neutron wave function on the surface does play a special role analogous to the role of Nilsson functions in the microscopic alpha decay theory of Mang and collaborators,[2] referred to in the introduction. Clearly, transfer amplitudes in angular configuration space are modulated by the odd-neutron wave function. In the angular momentum representation of the Alder-Winther-deBoer method we must make a Legendre transformation to get the closest-approach transformation matrix elements $T_{I\,I'}$, thus,

$$T_{I\,I'} = \int Y_{I0}^{*}\, a_{abs}(x)\Psi_{Nils}\,(R_{\ell},x)\; Y_{I'0}\; dx\; d\phi \tag{3}$$

The matrix expression is of the same form as the Fröman matrix [4]. For angular wave function of the $\frac{1}{2}^{+}$ [631] neutron orbital we have used simply the original tabulation by Nilsson [5] for diagonalization within one oscillator shell (N=6). The wave function at the $\eta = 6$ deformation chosen is as follows, in the original $(N\ell\Lambda|$ representation:

$$\Psi_{Nils+} = 1.0R_6Y_{60} + 0.879R_4Y_{40} - 2.021R_2Y_{20} - 1.712R_0Y_{00} \tag{4a}$$

$$\Psi_{Nils-} = -2.746R_6Y_{61} + 2.621R_4Y_{41} + 2.034R_2Y_{21} \tag{4b}$$

where the numbers are from Nilsson's table of coefficients, not normalized, and where Y_{LM} are spherical harmonics. The R_L functions are 6th oscillator shell radial wave functions

evaluated at the turning radius for the s-state (9.8 fm). Rather than using the Laguerre polynomial radial wave functions for the 3-dimensional harmonic oscillator we have calculated numerically by the "shooting method" the radial wave functions in a spherical Woods-Saxon potential of size appropriate to ^{239}Pu, but without spin-orbit coupling. These radial wave functions R_L(9.8 Fm) are 0.248, 0.216, 0.154, and 0.0750 for L = 0, 2, 4, and 6, respectively. The shell-model energies in our calculation correspond fairly well with the average shell model orbital energies of spin-orbit partners in Nilsson's calculation in the spherical limit. Here we have separated the intrinsic-spin-up components (+) from the spin-down components (-), since we must separately calculate probabilities for the two spin projections and add them, rather than adding amplitudes. In principle, one could perform the neutron-transfer experiment on a polarized ^{239}Pu target and measure the polarization in the final ^{91}Zr product; hence, we must calculate and add probabilities for the separate spin projections. Fig. 4 plots the surface amplitude factors vs. $\cos\theta$. The absorption factor (top curve) cuts the contribution at the poles to ~60% of their values at the equator. The lower curves are products of a_{abs} and the two spin component wave functions. The Nilsson functions have major lobes either side of nodes around $\cos\theta$ = 0.3 (spin up) and $\cos\theta$ = 0.45 (spin down).

Fig. 5 shows the theoretical rotational population patterns for the ^{90}Zr lab energy of 500 MeV, backscattering angle 140°, the mean scattering angle in the experiment, soon to be reported [8]. We used the Nilsson wave function for the deformation value of $\eta = 6$, which corresponds roughly to ß = 0.3 somewhat larger than the experimental deformation. We do not show the results here, but calculations for deformations of $\eta = 4$ were also performed and were found to resemble those for $\eta = 6$. It is seen that the spin-up

component of transfer gives a rotational population predominantly in a peak near the pure Coulomb excitation rainbow maximum around spin 18. The spin-down component predominantly populates a peak at spin 10. We do not show here the plots for other scattering angles and beam energies, but suffice it to say that the ratio of heights of the spin-10 and spin-18 peaks is sensitive to these parameters. The higher beam energies and/or scattering angles mean closer approach and more optical model absorption of high-latitude amplitudes. This, in turn, is manifested by a decrease in the spin-18 peak relative to the spin-10.

Discussion

It is interesting to consider what would be observed in some idealized cases. In this we use the semiclassical orbital concepts embodied in the pioneering work of Miller and George [13] for atomic-molecular systems and the early nuclear applications [14]. Even though we use these semiclassical pictures for visualization, we now rely on our modifications of the older time-dependent-Schrödinger equation approach of Alder, Winther and deBoer [9] for numerical calculations. Consider Nilsson orbitals in some large single-j shell. For the highest orbital in a prolate deformation, $\Omega = j$. This is a "pancake" orbital, with a single lobe on the equator. Only trajectories approaching the equator will be effective for transfer, and since the quadrupole torque vanishes at the equator, only low-rotational states should be populated. Likewise, the lowest-energy orbital in the j-shell will have its major lobe along the cylindrical symmetry axis, with minor lobes at finite angles. Again, low-spin final states should be preferred. If the transferred neutron is from an intermediate-Ω orbital, flat in energy with respect to increasing quadrupole deformation, the major lobe will be near 55°, the zero of $P_2(\cos\theta)$, and near the angle of maximum

torque (45°). In this case one should expect favoring of high-spin final states, even more so than rotational inelastic scattering, where all orientations contribute. There could also be interesting interference effects for neutron orbitals with nodes near 45°, in such cases high-spin population should be suppressed, and interference structure for intensities of reversed phase from Coulomb excitation. The $\frac{1}{2}^+$ [631] wave function we treat have major lobes near 45°(cos (θ) = .7), so high spins are enhanced.

There are obviously many ways to modify and improve these exploratory calculations, but we believe the essential features of the calculation will remain. It seems clear that the sensitivity to nuclear optical effects at these energies so near the top of the barrier may obscure effects of the neutron Nilsson function. Transfer experiments at lower energies would be cleaner to treat theoretically. Perhaps the next-generation of 4π gamma detector arrays, such as Gammasphere and Euroball, can facilitate n-transfer heavy-ion work on deformed nuclei at lower energy. Much of interest also to further test the theoretical methods here would be 1n transfer studies on even-even targets.

We see that Hans-Jörg Mang's early microscopic treatments in tunneling processes take on new relevance in contemporary heavy-ion transfer reaction theory. The prospects of further advances along these lines seem bright.

Acknowledgements

The main support for this research came from the Director Office of Energy Research, Division of Nuclear Physics of the Office of High Energy and Nuclear Physics of the U.S. Department of Energy under contract DE-AC03-76SF00098. We acknowledge also

the essential travel support of a U.S.-Brazil cooperative research grant INT-8382853 of the U.S. National Science Foundation and the Brazilian Conselho Nacional de Pesquisas e Desenvolvimento Cientifico.

References

1. H.J. Mang, Zeits f. Physik 148 (1957) 572; Sitzungsberichte der Heidelberger Akademie der Wissenschaften (1959) 299. H.J. Mang, Phys. Rev. 119 (1960) 1069.

2. H.J. Mang and J.O. Rasmussen, Mat. Fys. Skr. Dan. Vid. Selsk. 2 (1962) no.3.

3. J.O. Rasmussen and B. Segall, Phys. Rev. 103 (1956) 1298.

4. P.O. Fröman, Mat. Fys. Skr. Dan. Vid. Selsk. 2, (1957) no. 3.

5. B.R. Mottelson and S.G. Nilsson Mat. Fys. Skr. Dan. Vid. Selsk. 1 (1959) no. 8; S.G. Nilsson, Mat. Fys. Medd. Dan. Vid. Selsk. 29 (1955) no. 16.

6. M.W. Guidry, R. Donangelo, J.O. Rasmussen, and J.P. Boisson, Nucl. Phys. A295 (1978) 482.

7. C.Y. Wu, X.T. Liu, S.P. Sorensen, R.W. Kincaid, M.W. Guidry, D. Cline, W.J. Kernan, E. Vogt, T. Czosnyka, A.E. Kavka, M.A. Stoyer, J.O. Rasmussen, and M.L. Halbert, Phys. Lett. 188B (1987) 25.

8. M.A. Stoyer, Ph.D. Thesis, University of California, Berkeley (in preparation, Oct. 1990).

9. K. Alder and A. Winther "Coulomb Excitation," Academic Press, New York (1966).

10. L.F. Canto, R. Donangelo, J.O. Rasmussen, P. Ring, and M.A. Stoyer, "Semiclassical Treatment of Nuclear Effects in Coulomb Excitation," Report IF/UFRJ 90/31, accepted Physics Letters B.

11. M.J. Rhoades-Brown, R. Donangelo, M.W. Guidry and R.E. Neese, Phys. Rev. C24 (1981) 2747.

12. L.F. Canto, R. Donangelo, R.S. Nikam, and P. Ring, Phys. Lett. 192B (1987) 4.

13. T.F. George and W.H. Miller, J. Chem. Phys. 56 (1972) 5668.

14. M.W. Guidry, H. Massmann, R. Donangelo, and J.O. Rasmussen, Nucl. Phys. A274 (1976) 183.

Figure Legends

Fig. 1. Calculated rotational state population patterns for pure Coulomb excitation of ^{238}Pu by ^{90}Zr at three different beam energies 480 MeV (open circles, solid lines), 500 MeV (solid circles, dashed lines), and 520 MeV (solid squares, dashed lines.) The calculations are all for 180° backscattering.

Fig. 2. Comparison of pure Coulomb excitation calculations for ^{239}Pu using experimental rotational state energies (open circles, solid lines) and using the fully-decoupled-neutron approximation with Coulomb excitation of ^{238}Pu, partitioning the intensities among the I ± 1/2 states by statistical weight 2I + 1. The calculation is for ^{90}Zr beam energy of 500 MeV and 180° backscattering.

Fig. 3. Rotational state populations calculated with the complex nuclear optical potential and effective-Z, effective-E approximation described in Ref.10. The collision partners are the same as in Fig. 1. The profound effects of the nuclear potential in suppressing high-spin population as well as the interference oscillations are clearly seen. The beam energy is that of experiment, 500 MeV, but adjusted to reproduce the distance of closest approach for a 140° scattering angle.

Fig. 4. Angle-dependent amplitude-modulation factors for the transfer calculation shown in Fig. 5. The attenuation factor a_{abs} is the top (dash-dot) curve. The lower two curves are the products of a_{abs} and the surface Nilsson wave functions of the $\frac{1}{2}^+$ [631] orbital (dotted, spin up; dashed, spin down).

Fig. 5. Calculated population patterns in ^{238}Pu from the 1-n transfer on ^{239}Pu by ^{90}Zr. The two spin-polarization components are shown separately along with their total populations. Here the Nilsson wave function for a deformation of $\eta = 6$ was used. The complex nuclear optical potential was included, as were effective parameters to adjust the orbital distance of closest approach in the calculated head-on collision to match that for the conditions of the experiment of ref. [8]. That is, an energy of 494 MeV with 180° backscattering was used to match the turning distance for 500 MeV with 140° backscattering.

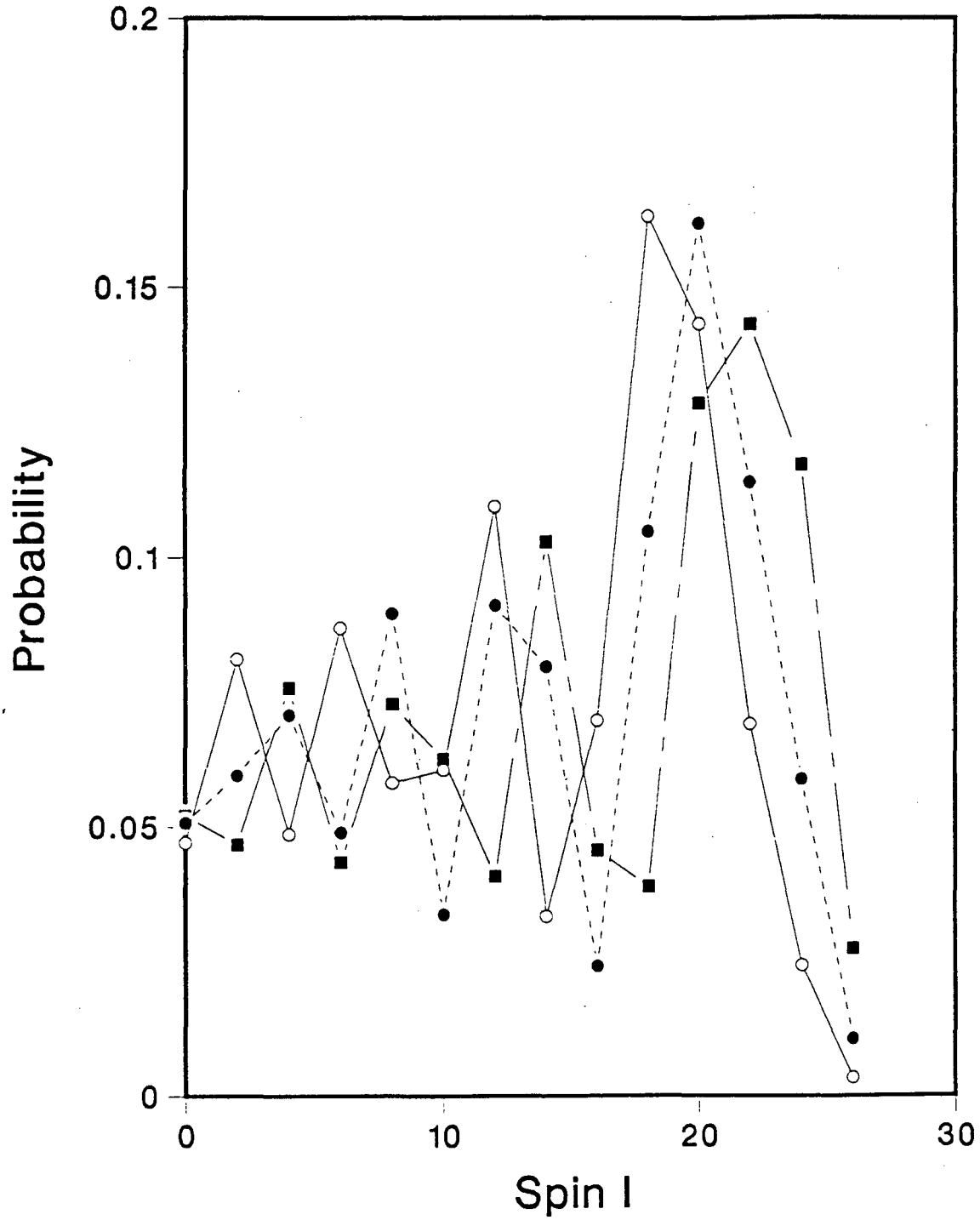

XBL 909-3287

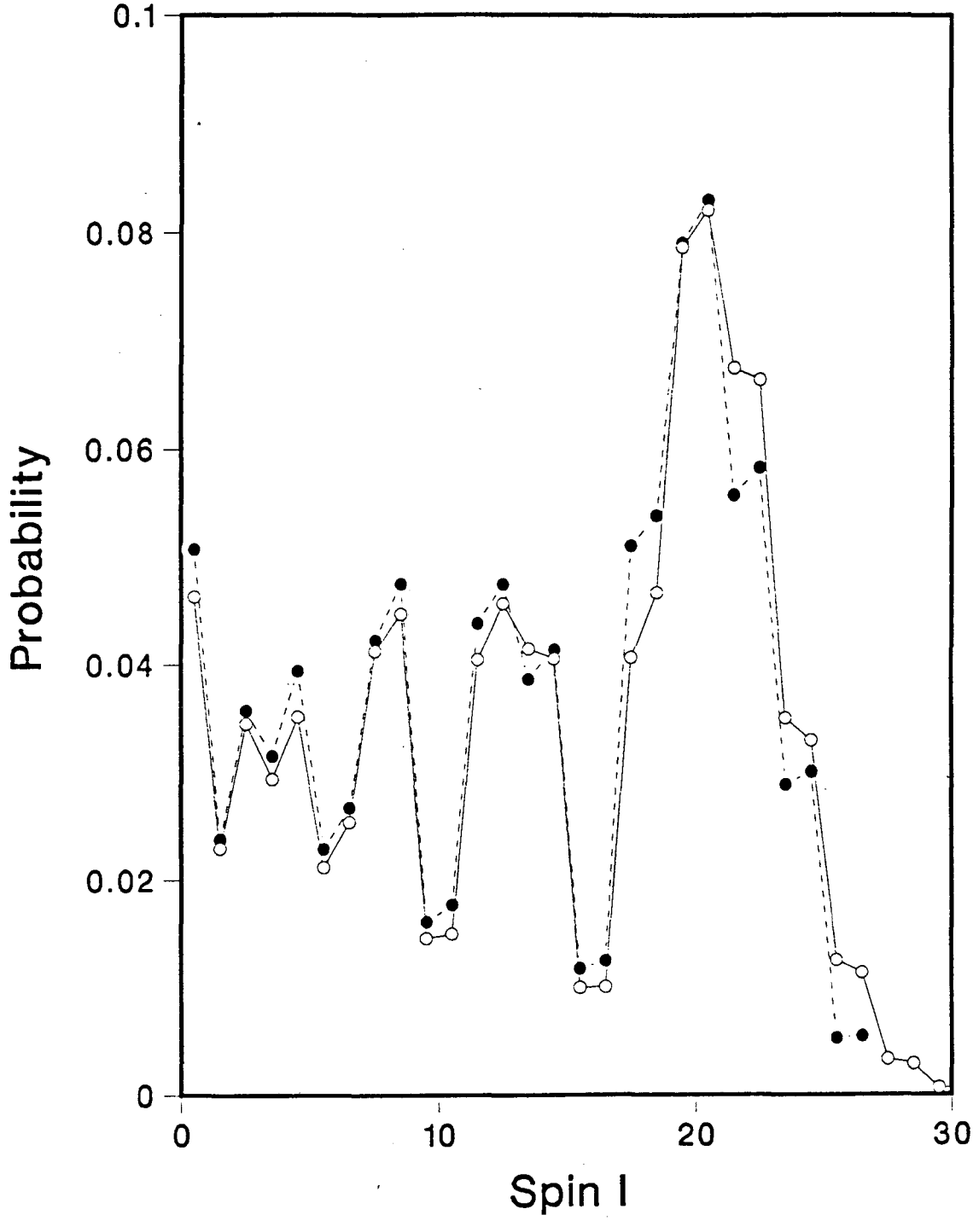

XBL 909-3288

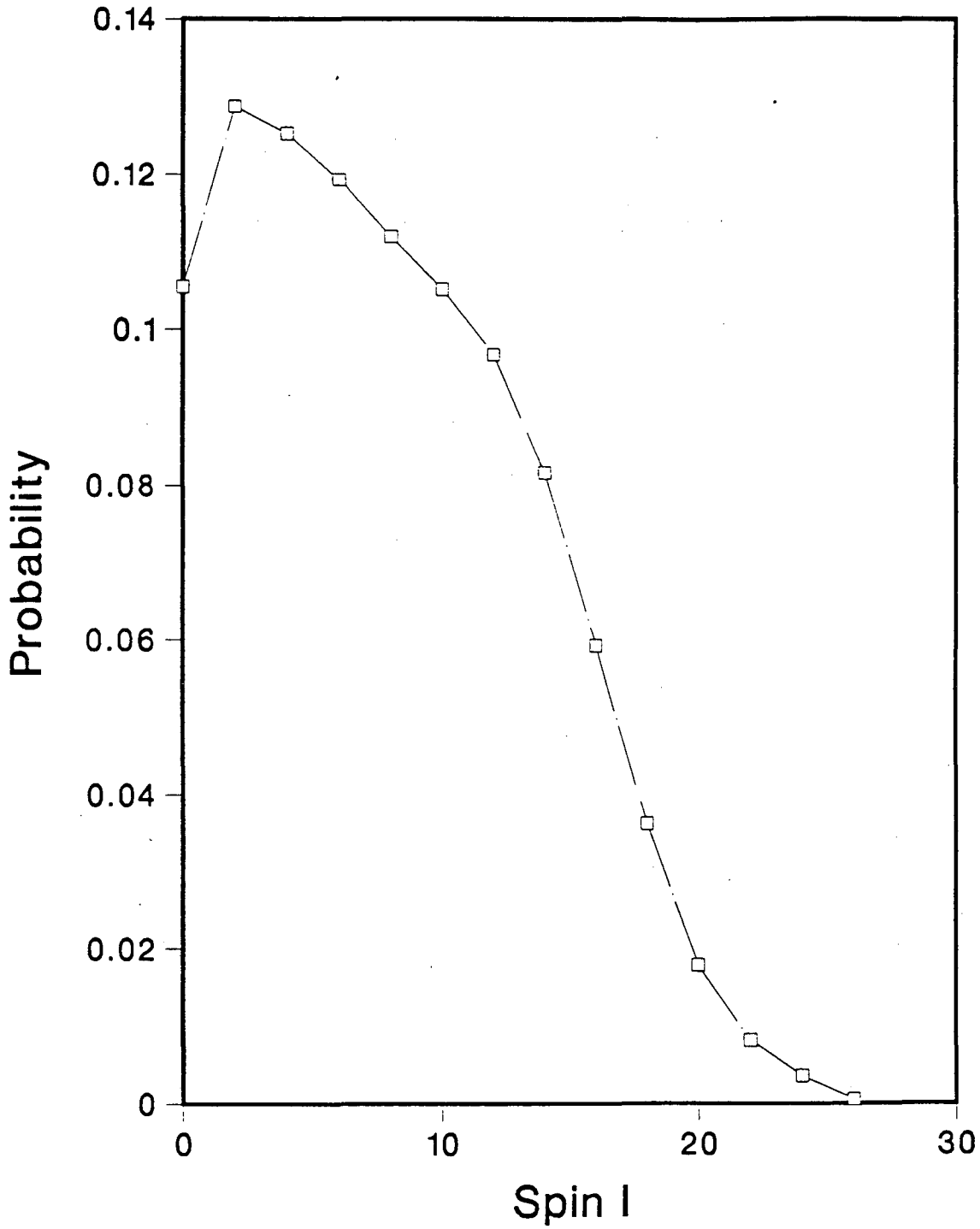

XBL 909-3289

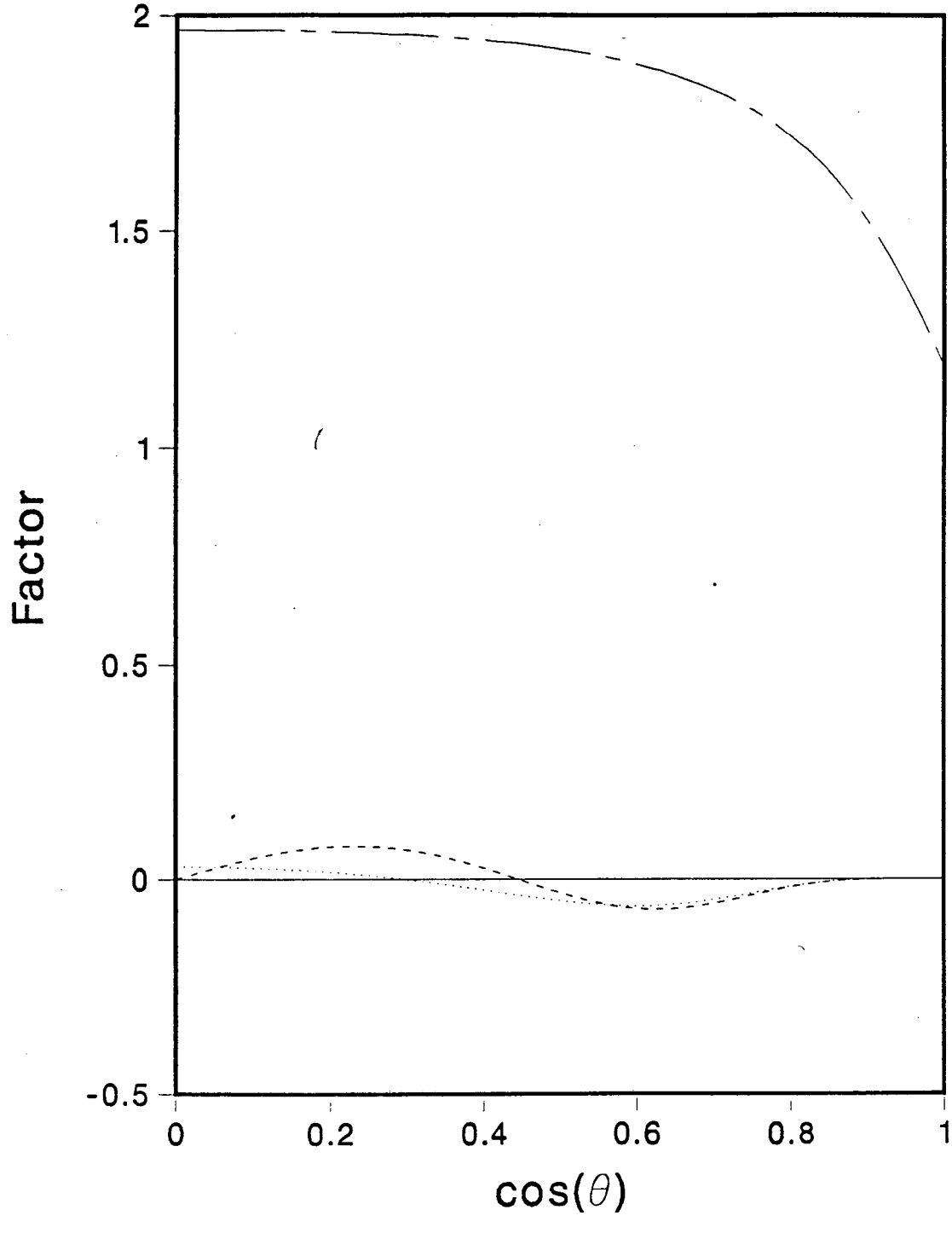

XBL 909-3290

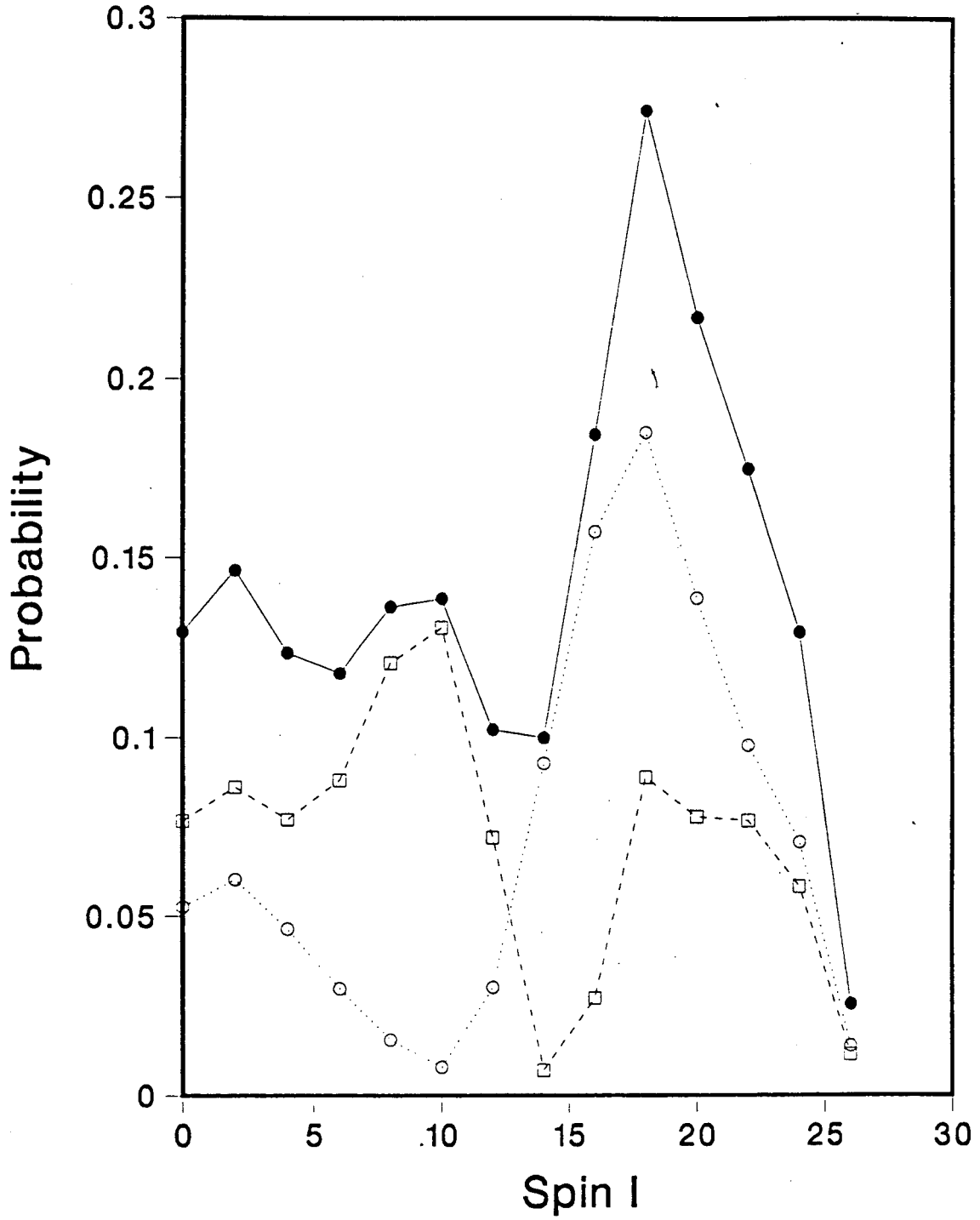

XBL 909-3291

LAWRENCE BERKELEY LABORATORY
UNIVERSITY OF CALIFORNIA
INFORMATION RESOURCES DEPARTMENT
BERKELEY, CALIFORNIA 94720